Modifying ceria (111) with a TiO_2 nanocluster for enhanced reactivity

Michael Nolan

Citation: The Journal of Chemical Physics **139**, 184710 (2013);
View online: https://doi.org/10.1063/1.4829758
View Table of Contents: http://aip.scitation.org/toc/jcp/139/18
Published by the American Institute of Physics

Modifying ceria (111) with a TiO_2 nanocluster for enhanced reactivity

Michael Nolan[a)]
Tyndall National Institute, University College Cork, Lee Maltings, Dyke Parade, Cork, Ireland

(Received 30 August 2013; accepted 21 October 2013; published online 11 November 2013)

Modification of ceria catalysts is of great interest for oxidation reactions such as oxidative dehydrogenation of alcohols. Improving the reactivity of ceria based catalysts for these reactions means that they can be run at lower temperatures and density functional theory (DFT) simulations of new structures and compositions are proving valuable in the development of these catalysts. In this paper, we have used DFT+U (DFT corrected for on-site Coulomb interactions) to examine the reactivity of a novel modification of ceria, namely, modifying with TiO_2, using the example of a Ti_2O_4 species adsorbed on the ceria (111) surface. The oxygen vacancy formation energy in the Ti_2O_4–CeO_2 system is significantly reduced over the bare ceria surfaces, which together with previous work on ceria-titania indicates that the presence of the interface favours oxygen vacancy formation. The energy gain upon hydrogenation of the catalyst, which is the rate determining step in oxidative dehydrogenation, further points to the improved oxidation power of this catalyst structure.
 [http://dx.doi.org/10.1063/1.4829758]

I. INTRODUCTION

Ceria is widely used in catalysis due to its oxygen storage capacity, OSC.[1–3] This is the ability of ceria to store and release oxygen depending on the reaction conditions. Under oxygen poor conditions, oxygen is released, reducing ceria. Under oxygen rich conditions, oxygen is taken up, healing the vacancy and reoxidising ceria. Oxygen vacancy formation and healing is intimately connected to the change in oxidation state of cerium from oxidised Ce^{4+} to reduced Ce^{3+},[4–6] the ease of which makes ceria a reducible metal oxide.

Of particular interest is the role of ceria in oxidation catalysis, e.g., for CO oxidation to CO_2[7–12] and for the oxidative dehydrogenation (ODH) of methanol to formaldehyde.[13–16] Over recent years, a great deal of work has examined how the reactivity of ceria in oxidation reactions can be enhanced.[17–31] In CO oxidation, which occurs by the Mars van Krevelen mechanism (CO removes lattice oxygen from CeO_2 and this oxygen is returned from the atmosphere or from reduction of NO_x species), the key step is the removal of oxygen from ceria. Thus, enhancing oxygen vacancy formation, by making its energy cost lower, can be of benefit by lowering the reaction temperature and improving the oxidative power of ceria.[31] There have been a number of theoretical studies elaborating upon this idea, and some experiments confirming this concept.[17–31]

Modifying ceria to promote reactivity is achieved in two approaches: substitution of a Ce^{4+} ion with another metal (so-called "doping") or modification of ceria with molecular sized metal nanoparticles or metal oxide structures. For doping, metals that lower the oxygen vacancy formation energy include Pt,[31] La,[30] Pd,[17] Ti,[29] and Au,[27,28] and this improves the activity for oxidation reactions. Modifying ceria (111) surfaces with small metal particles is also intensively studied, with well-known examples being Au, Pt, and Pd nanoparticle modified ceria.[31–35] However, the enhanced catalytic activity does not necessarily arise from a lowering of the oxygen vacancy formation energy, as demonstrated in a first principles density functional theory with Hubbard U correction (DFT+U) study of Cu adsorption at the (111) surface of ceria.[34] In this study, an adsorbed Cu atom actually inhibited oxygen vacancy formation. For a notable positive effect of modifying ceria with metal nanoparticles, the work in Ref. 35 where a ceria nanoparticle is modified by a Pt_8 nanocluster is of note.

Modifying ceria with small, molecular sized, metal oxide structures has been of particular interest in oxidation reactions. A particularly well studied example is VO_x supported on ceria, while VO_x modified TiO_2 has also been investigated.[36–42] The reactivity of VO_x-modified CeO_2, using the oxygen vacancy formation energy as an activity descriptor, is enhanced compared to the individual metal oxides, highlighting the synergy of ceria and VO_x in determining the reactivity. Modifying ceria (111) with VO_x results in formation of Ce^{3+} and fully oxidised V^{5+}[41,42] and oxygen vacancy formation produces Ce^{3+} ions but does not change the oxidation state of vanadium, so that the flexibility of ceria's oxidation state plays an important role.

In a notable example, the ODH of methanol to formaldehyde was investigated with DFT+U[41,42] calculations and with temperature programmed desorption (TPD) experiments on VO_x modified CeO_2(111) films.[40,42] In the ODH of methanol on VO_2–CeO_2, a TPD peak for formaldehyde desorption is found at 370 K. This peak is at significantly lower temperature than for unmodified CeO_2, where it is found at 565 K.

In the ODH of alcohols and alkanes on metal oxides, the rate limiting step is a redox reaction in which the C–H bond is cleaved.[42–44] In an alkane, the initial binding to an oxide is generally van der Waals, but methanol adsorption can lead to dissociative adsorption, forming hydroxyl and

a)E-mail: michael.nolan@tyndall.ie

methoxy groups at the surface. Hydrogen is abstracted from the surface bound methoxy group to make an O–H bond with surface oxygen,[42–44] which reduces a metal centre.

In studying the activity of VO_x-modified CeO_2 for methanol ODH, the DFT+U simulations focussed on the oxygen vacancy formation energy and the hydrogen adsorption/Ce reduction energy as the descriptors of the reactivity of the model catalyst structures, relating these to the reaction energy through the Bronsted-Evans-Polyani (BEP) principle,[45,46] which has been discussed in, e.g., the work of Metiu and co-workers.[47] Thus, the lower the oxygen vacancy formation energy is or the more exothermic the hydrogen adsorption energy, then the lower will be the energy barrier for these rate limiting steps allowing modifications to enhance the reactivity of ceria (111) to be identified.[47,48]

Vanadia modified ceria (111) has been well studied and DFT+U simulations of this system have been shown to be reliable in identifying the reasons for the enhanced activity of modified ceria over unmodified ceria. It is therefore interesting to use DFT+U simulations to examine if there are other possible modifications of ceria with molecular sized transition metal oxides that will also enhance reactivity for oxidation reactions or if this would only be the case for vanadium. This paper presents DFT+U simulations of the reactivity of a model system, that is, the CeO_2 (111) surface modified with a supported TiO_2 nanocluster. We choose a nanocluster with composition Ti_2O_4 as a representative model TiO_2 nanocluster. We note that for vanadia modified ceria, the oxide is modified by very small, molecular sized structures such as VO_2, V_2O_5,[40] and rutile TiO_2 (110) modified with small[49–54] and more recently, large particles[55] CeO_2/Ce_2O_3 species has been examined. In Ref. 55, the authors find that, contrary to their work on smaller ceria nanoclusters supported on rutile (110), mixing of Ce and Ti occurs. Thus, the Ti_2O_4 cluster used in this study to modify the ceria (111) surface can be considered a reasonable model structure. We do not examine any intermixing of Ti and Ce, as the work in Refs. 49–54 would indicate that, for clusters at this size, intermixing will not take place.

We investigate if this modification to ceria, can enhance its reactivity by examining

(i) the oxygen vacancy formation energy;
(ii) the adsorption of hydrogen; and
(iii) the adsorption of methanol and formation of formaldehyde.

We compare this model system with both the bare CeO_2 surface and the general findings for vanadia modified CeO_2. Modifying CeO_2 with the Ti_2O_4 nanocluster results in

- A reduction in the oxygen vacancy formation energy compared with the bare (111) surface.
- A more exothermic H adsorption energy compared to the bare (111) surface.
- Exclusively dissociative adsorption of methanol and formation of formaldehyde.

Thus, this work identifies the modification of CeO_2 (111) with TiO_2 as a potentially useful model catalyst system for oxidative reactions.

II. METHODOLOGY

To model the ceria (111) surface, we use a three-dimensional periodic slab model and a plane wave basis set to describe the valence electronic wave functions within the VASP.5.2 code.[56] The cutoff for the kinetic energy is 396 eV, which we have used in a number of studies on ceria; however, as a check, we have also performed some calculations with a 500 eV cutoff energy. This change to the plane wave cutoff energy modifies the vacancy formation energies given in Sec. III B by no more than 0.05 eV. For the core-valence interaction, we apply Blöchl's projector augmented wave (PAW) method,[57] with Ce described by 12 valence electrons, Ti by 4 valence electrons, and oxygen by 6 valence electrons. We use the PBE approximation to the exchange-correlation functional.[58] k-point sampling is performed using the Monkhorst-Pack scheme, with a $(2 \times 2 \times 1)$ sampling grid.

To consistently describe the electronic states of reduced Ce^{3+} and Ti^{3+} in CeO_2 and in TiO_2, we have used the DFT+U approach,[59,60] which has been successfully applied to both CeO_2 and TiO_2.[61–63] DFT+U adds a Hubbard U correction to describe the localised electrons in reduced metal cations such as Ce^{3+} and Ti^{3+}. These oxidation states can result from formation of oxygen vacancy defects, doping, or hydrogen adsorption. For CeO_2, values of U in the range 4–5 eV are generally reasonable,[9,10,34,41] and we used $U = 5$ eV for the Ce 4*f* states. For TiO_2, values of U in the range 3–5 eV are reasonable[51,62] and we apply $U = 4.5$ eV to the Ti 3*d* states. A number of authors have advocated using an additional +U correction on the O 2*p* states in describing stoichiometric ceria[64] and hole forming defects in ceria,[65] however, we do not apply this correction in this work. While DFT+U fixes many problems with approximate DFT in describing partially occupied electronic states, it still shows some issues and quantities such as formation energies tend to vary with values of U. However, we use a robust set of DFT+U parameters that have also been used in the literature and are interested in how modifying ceria surfaces with a TiO_2 nanocluster can change the electronic structure and reactivity compared to the corresponding bare surface with the same computational scheme.

The (111) surface is a Tasker type II surface,[66] terminated by oxygen, with neutral O–Ce–O trilayers normal to the surface and we use a 12 atomic layer thick (4×4) surface supercell expansion, large enough to allow for adsorption of an essentially isolated TiO_2 cluster and a vacuum gap of 12 Å is used, while the bottom trilayer is fixed and all other layers are allowed relax. The convergence in the wavefunction relaxation is 0.0001 eV, while the ionic relaxation is converged when the forces on the atoms are less than 0.02 eV/Å. Fermi level smearing with the Methfessel Paxton scheme is applied, with $\sigma = 0.1$ eV; total energies used in the calculation of adsorption and vacancy formation energies are taken from extrapolation of σ to 0. All calculations are spin polarised.

The bare ceria surface, the free Ti_2O_4 cluster, and the Ti_2O_4 modified (111) surface are calculated with the same set of technical parameters and within the same supercell to

ensure consistency between calculations. To study cluster adsorption, the Ti_2O_4 cluster is positioned at a number of configurations at the surface and a full relaxation is performed within a fixed supercell. The adsorption energy is computed from

$$E^{ads} = E((Ti_2O_4) - CeO_2) - \{E(Ti_2O_4) + E(CeO_2)\}, \quad (1)$$

where $E((Ti_2O_4)–CeO_2)$ is the total energy of the Ti_2O_4 cluster supported on the CeO_2 surface, and $E(Ti_2O_4)$ and $E(CeO_2)$ are the total energies of the free Ti_2O_4 cluster and the bare surface; a negative adsorption energy signifies that cluster adsorption is stable. For oxygen vacancies, we remove oxygen atoms from both the adsorbed cluster and from the CeO_2 surface and relax. We compute the oxygen vacancy formation energy, E^{vac}, from

$$E^{vac} = E((Ti_2O_3) - CeO_2) - \{E(Ti_2O_4 - CeO_2) + 1/2E(O_2)\}, \quad (2)$$

$$E^{vac} = E((Ti_2O_4) - CeO_{2-x}) - \{E(Ti_2O4 - CeO_2) + 1/2E(O_2)\}, \quad (3)$$

where Eq. (2) signifies removal of oxygen from the Ti_2O_4 cluster and Eq. (3) signifies removal of oxygen from the CeO_2 surface.

The adsorption energy for a hydrogen atom at the Ti_2O_4–CeO_2 structure (resulting from homolytic cleavage of H_2) is computed from

$$E_H^{ads} = E((H - Ti_2O_4) - CeO_2) - \{E(Ti_2O_4 - CeO_2) + 1/2E(H_2)\}, \quad (4)$$

where similar to Refs. 41 and 42, we reference to half the total energy of H_2 and we find hydrogen adsorption at the TiO_2 nanocluster is more stable than at the CeO_2 surface.

Finally, we consider both molecular and dissociative adsorption of methanol at the Ti_2O_4–CeO_2 system, with methanol adsorption energies computed from

$$E_{CH_3OH}^{ads} = E((CH_3OH - Ti_2O_4) - CeO_2) - \{E(Ti_2O_4 - CeO_2) + E(CH_3OH)\}. \quad (5)$$

Further details on methanol adsorption modes are given in Sec. III D.

III. RESULTS

A. Adsorption structures of Ti_2O_4 on the CeO_2 (111) surface

A number of adsorption structures for Ti_2O_4 on the ceria (111) surface (in a (4×4) surface supercell) were constructed and relaxed. The most stable adsorption structure is shown in Figure 1 with an adsorption energy of −4.30 eV, indicating a strong interaction between the surface and the Ti_2O_4 cluster. In the remainder of the paper, we denote the Ti_2O_4–CeO_2 (111) structure as **Ti_2O_4@(111)**.

In discussing the geometry, Ti^c signifies cluster Ti atoms, O^s and O^c signify surface and cluster oxygen and Ce is only present in the surface. When the Ti_2O_4 nanocluster adsorbs

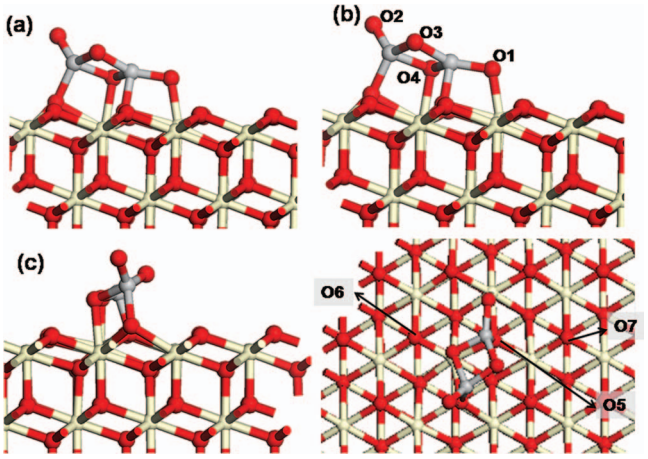

FIG. 1. (a) and (c) Adsorption structure of the Ti_2O_4 cluster supported at the (111) ceria surface. (b) Numbering of the oxygen atoms removed in forming the oxygen vacancies; O1–O4 are in the nanocluster and O5–O7 are in the surface. In this, and subsequent figures, Ce is white, Ti is grey, and O is red.

at the (111) surface, two cluster oxygen atoms (O1 and O4 in Figure 1) bind with Ce on the surface. A third oxygen in the nanocluster remains two coordinated without binding to the surface and the final oxygen atom in the cluster is a terminal oxygen. Of the oxygen atoms in the cluster that bond to the surface, one oxygen atom is two-coordinated and the other is three-coordinated. Surface Ce atoms bind to cluster oxygen with distances of 2.25 Å (O1, a two coordinated O^c) and 2.42 Å (O4, a three coordinated O^c). The same Ce atoms also display elongated surface Ce^s–O^s distances of 2.40–2.59 Å. The two Ti^c atoms bind to different surface oxygen atoms and are now four coordinated. One Ti^c has a Ti^c–O^c distance of 1.70 Å to the terminal oxygen in the nanocluster (typical of terminal Ti–O distances[67]). This Ti^c further binds to a surface oxygen with a distance of 2.01 Å and as a consequence of the interaction, this oxygen is displaced from its surface site by 0.45 Å, breaking the previous bond to a surface Ce^s (Ce^s–O^s distance of 2.89 Å). The Ti^c–O^c distances in the nanocluster range are 1.86–2.02 Å, which are lengthened by up to 0.15 Å from the free cluster. Ti^c to O^s distances are in the range of 1.86–1.91 Å, with these oxygen pulled out of the surface by 0.1 Å. The remainder of the (111) surface is not perturbed by the Ti_2O_4 cluster, indicating a local interaction between the surface and the nanocluster.

The electronic density of states projected onto Ti 3*d*, Ce 4*f* states, and O 2*p* states of the nanocluster and the ceria (111) surface (the PEDOS) are shown in Figure 2(a). The PEDOS is typical of fully oxidised TiO_2 and CeO_2, with no evidence of reduced Ti^{3+} or Ce^{3+} as a result of any charge transfer from the cluster to the surface or vice versa. For both oxides, the valence band is dominated by the O 2*p* states, with typical Ti 3*d* and Ce 4*f* contributions also present. The valence band edge is composed of O 2*p* states from the nanocluster, with the surface derived O 2*p* states lying 0.4 eV lower. The empty Ce 4*f* states lie 1.5 eV above the VB edge, and the empty Ti 3*d* states are a further 0.25 eV higher in energy. Thus, the original energy gap between the CeO_2 valence band and the empty Ce 4*f* states has been narrowed by 0.4 eV upon deposition of the TiO_2 nanocluster at the (111) surface which

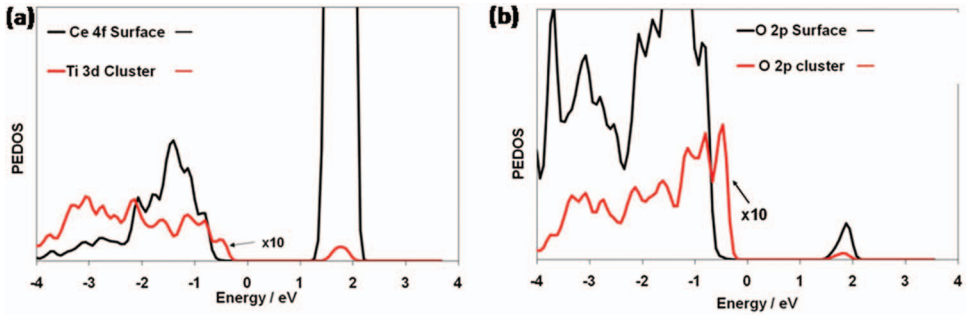

FIG. 2. (a) Ce 4*f*, Ti 3*d* and (b) nanocluster and surface O 2*p* PEDOS for Ti_2O_4 supported on the ceria (111) surface. The Ti_2O_4 contributions to the PEDOS are multiplied by 10 to enable a comparison with the CeO_2 PEDOS. The zero of energy is the Fermi level.

provides an interesting mechanism for tuning the light absorption characteristics in CeO_2, e.g., see Ref. 67.

B. Reactivity of Ti_2O_4–CeO_2 structure

1. Oxygen vacancy formation

As discussed in the Introduction, in oxidation reactions that follow the MvK mechanism, the oxygen vacancy formation energy is a useful descriptor of the activity of a catalyst in CO oxidation.[41,42,45] Thus, for the example of doped ceria surfaces, dopants that reduce the energy cost needed to form an oxygen vacancy have been investigated and examples of dopants that enhance the oxidative power of ceria include Ti,[35] Pt,[31] and La.[30] The effect of a VO_2 species adsorbed at the ceria (111) surface on promoting oxidative power is demonstrated by a reduction of around 1 eV in the computed oxygen vacancy formation energy compared to the bare (111) surface.[41,42] To confirm this, in experiments, a lower temperature TPD peak was observed for the ODH of methanol on VO_2-modified CeO_2.[40,42]

We have previously computed for the bare CeO_2 (111) surface an oxygen vacancy formation energy of 2.70 eV from our DFT+U setup.[59] To examine the effect of modifying ceria (111) with a TiO_2 nanocluster on the oxygen vacancy formation energy, we have removed a number of oxygen atoms from both Ti_2O_4 and the (111) surface, to examine which oxygen sites are the most favourable for oxygen vacancy formation; see Figure 1(b). Table I presents the computed oxygen vacancy formation energies within our present DFT+U scheme. The atomic structure of the most stable oxygen vacancy structures with the vacancy found in the Ti_2O_4 cluster and in the ceria surface are shown in Figure 3.

For Ti_2O_4@(111), the most stable oxygen vacancy site is a terminal cluster oxygen atom, indicated by O2 in Figure 1(b). The most stable oxygen vacancy site in the (111) surface is a surface oxygen atom lying under the Ti_2O_4 cluster, indicated as O5. These oxygen vacancy sites show a reduction of 0.65 eV (O2) and 0.49 eV (O5) in the oxygen vacancy formation energy compared to the bare (111) surface. Such a reduction in the oxygen vacancy formation energy over the bare surface, while not as dramatic as found for VO_2-modified ceria, will still be useful for enhancing the oxidative power of ceria. In Ref. 55, the formation of oxygen vacancies is enhanced by the ceria-titania interface and the findings of Refs. 41, 42, and 55 together with the present work strongly indicate that the presence of an oxide-oxide interface is beneficial for the formation of oxygen vacancies in reduced metal centres.

Examining the atomic structure for Ti_2O_4@(111) with the most stable oxygen vacancy sites, we find that when the surface oxygen O5 is removed, oxygen O1 in the Ti_2O_4 nanocluster moves during the relaxation to fill the surface oxygen vacancy site. This structure is in fact very similar to the O1 vacancy site, with an energy difference of only 0.08 eV (Table I). The remaining surface oxygen vacancy sites in the

TABLE I. Computed oxygen vacancy formation energies (E^{vac}, in eV) for one oxygen vacancy in the Ti_2O_4–CeO_2 structures and the vacancy formation energy of the bare surface is included for comparison. The oxygen site numbering follows Figure 1(b). The figures in boldface indicate the most stable oxygen vacancy sites.

Ti_2O_4@CeO_2 (111)			
O vacancy site	E^{vac} (eV)	O vacancy site	E^{vac} (eV)
1	2.29	5	**2.21**
2	**2.05**	6	2.56
3	3.54	7	2.31
4	3.62		
Bare (111)		2.70	

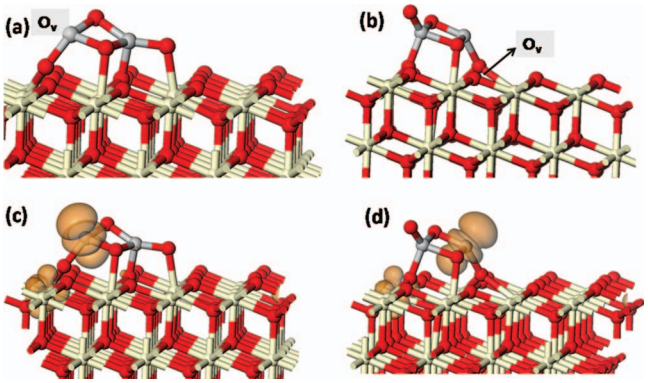

FIG. 3. The atomic structure of the most stable oxygen sites and their excess spin density for Ti_2O_4 supported on the ceria (111) surface. (a) O^c vacancy site on the (111) surface, (b) O^s vacancy site on the (111) surface, (c) spin density for O^c vacancy site on the (111) surface, and (d) spin density for O^s vacancy site on the (111) surface. The oxygen vacancy site is indicated by "O_v" and the orange spin density isosurfaces enclose spin densities of 0.02 electrons/Å^3.

(111) surface are true surface oxygen vacancies, and while these sites do show a smaller oxygen vacancy formation energy than the bare surface, they still lie higher in energy than the most stable surface and cluster vacancy sites.

Figure 3 also shows the resulting excess spin density for the two most stable oxygen vacancies. With two electrons released by formation of a neutral oxygen vacancy, there is the possibility that Ti^{4+} or Ce^{4+} can be reduced to Ti^{3+} or Ce^{3+} and the spin density shows that for Ti_2O_4@(111), one surface Ce atom and one cluster Ti atom are reduced to Ce^{3+} and Ti^{3+}. This is irrespective of whether the oxygen vacancy comes from Ti_2O_4 or from the (111) surface. This is similar to our finding for TiO_2 nanoclusters supported on the rutile TiO_2 (110) surface, where generally one Ti atom in the nanocluster and one Ti atom in the surface are reduced to Ti^{3+} after oxygen vacancy formation.[67] For reduced Ce^{3+} and Ti^{3+}, the calculated net Bader charges[68] are 9.86 electrons on Ce^{3+} (with a computed spin magnetisation of 0.97 electrons) and 1.86 electrons on Ti^{3+} (spin magnetisation of 0.89 electrons). These are typical for reduced Ce^{3+} and reduced Ti^{3+}.

The reduced Ti and Ce ions show localised changes in their corresponding Ti–O and Ce–O distances after oxygen vacancy formation, and some of these changes are of interest. For example, in the (111) surface with a cluster oxygen vacancy, the Ti^c–O^c distances involving the Ti^{3+} species are 1.93 and 1.94 Å, with Ti^c–O^s distances of 1.93 Å. However, compared to the stoichiometric structure, these distances are in fact shorter by 0.08 Å. The usual expectation upon forming reduced Ti^{3+} species is a geometry distortion that lengthens the Ti^{3+}–O distances. We attribute this result to the reduced coordination of the Ti^c after oxygen vacancy formation, which shortens the Ti–O distances and competes with the lengthening of Ti^{3+}–O distances usually seen in, e.g., rutile TiO_2 surfaces,[61] so that the final Ti^{3+}–O distance is a balance between the two. In the same structure, the Ce^s–O^s distances for the reduced Ce^{3+} species are around 2.49 Å, typical of the Ce–O bond length elongation found for reduced Ce^{3+} species.[63] For the most stable surface oxygen vacancy structure, O5, similar Ti^{3+}–O and Ce^{3+}–O distances are found compared to the nanocluster oxygen vacancy, which is not unsurprising since the reduced Ti^{3+} ion is in a similar environment to that in which the oxygen vacancy is present in the nanocluster.

C. Probing reactivity to hydrogenation: Adsorption of hydrogen at T_2O_4–CeO_2 (111)

To examine the reactivity of Ti_2O_4–CeO_2 for the ODH reaction, we have modelled the adsorption of a hydrogen atom at Ti_2O_4@(111); this facilitates at least a qualitative comparison with existing work on VO_2-modified ceria(111). As discussed in the Introduction, the hydrogenation energy at the metal oxide catalyst is a good descriptor of the activity of a catalyst for ODH reactions.[41,42,47,48] We consider homolytic dissociation of H_2 so that when a H atom adsorbs at the Ti_2O_4@(111) structure it can donate an electron to Ti_2O_4 or CeO_2, with formation of reduced Ti^{3+} or Ce^{3+}.

Figure 4 shows the atomic structure of H adsorption at two different sites on the Ti_2O_4 cluster; adsorption of H at

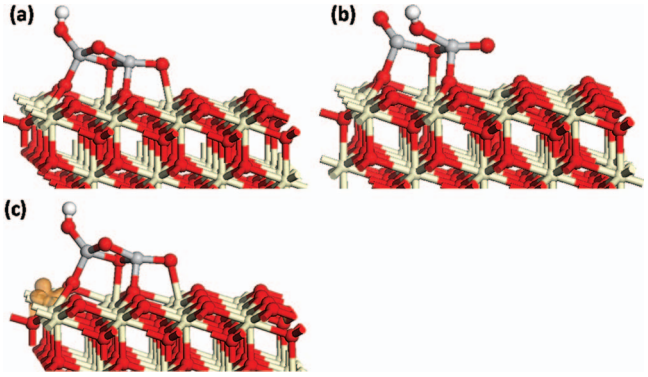

FIG. 4. Adsorption structure of a hydrogen atom adsorbed at Ti_2O_4–CeO_2 (111). (a) The most stable adsorption site, (b) the next most stable adsorption site, (c) the excess spin density in the most stable structure showing the presence of a Ce^{3+} ion; orange spin density isosurfaces enclose spin densities up to 0.02 electrons/Å^3.

the Ti_2O_4 cluster is more stable than adsorption on the (111) surface. The adsorption energy of H at the most stable site, titanyl oxygen O2 (Figure 4(a)), is −1.70 eV, referenced to half the total energy of a H_2 molecule. The other adsorption site, 2-coordinated oxygen O1 (Figure 4(b)) has an adsorption energy of −1.10 eV. In Ref. 41, using PBE+U, with U = 4.5 eV a H atom adsorbs at the surface VO_2 species, with an energy gain of 1.21 eV. Using the energetics of H adsorption as a descriptor, modifying the CeO_2 (111) surface with a TiO_2 nanocluster will enhance reactivity over the bare surface, in a similar fashion to VO_2-modified CeO_2.

In the most stable H adsorption structure, H binds to the titanyl oxygen O2 in the Ti_2O_4 nanocluster, which is a reasonable site for H atom adsorption. The resulting O–H bond distance is 0.97 Å, and the Ti–O distance to cluster oxygen is now 1.89 Å, which is an elongation of 0.19 A over corresponding Ti–O distances in the bare Ti_2O_4@(111) structure.

The excess spin density is shown in Figure 4(c) and demonstrates that one surface Ce ion is reduced to Ce^{3+} as a result of transfer of the electron from the H atom to the surface. The computed net Bader charge on this Ce ion is 9.85 electrons and the spin magnetisation is 0.97 electrons, both consistent with formation of a reduced Ce^{3+} species. This Ce ion has elongated Ce–O distances of 2.42, 2.44 (×2), and 2.48 Å to neighbouring surface oxygen, which are consistent with a Ce^{3+} species.

D. Adsorption and reaction of methanol at Ti_2O_4–CeO_2 (111)

To further examine the effect of the CeO_2 (111) surface modification with Ti_2O_4, we have studied the adsorption of methanol at this structure and subsequent formation of formaldehyde. The adsorption of methanol at the perfect (111) surface has previously been studied in Refs. 69–71. Beste *et al.*[70] found two adsorption modes on the perfect (111) surface from DFT+U calculations: molecular and dissociative as methoxy and hydroxyl, with adsorption energies of −0.76 eV and −0.08 eV. Mei *et al.*[71] also used DFT+U to study methanol adsorption at the clean (111) surface. These authors find a coverage dependent adsorption process. At

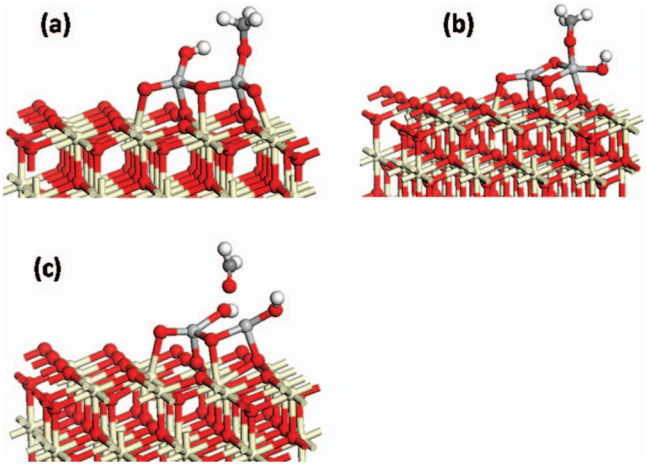

FIG. 5. Relaxed atomic structures for methanol adsorption at Ti_2O_4@CeO_2(111): (a) Final structure starting from molecular adsorption, (b) dissociative adsorption with the O–H bond broken, and (c) dissociative adsorption with the methyl C–H bond broken.

0.25 ML, dissociative adsorption via breaking of a C–H bond in methyl (giving hydroxymethyl CH_2OH) is more favourable and as coverage increases, molecular adsorption dominates. O–H bond breaking is the next most stable dissociative adsorption mode, followed by C–O bond breaking. These studies have not applied dispersion-corrected functionals to the adsorption of methanol at ceria (111). However, dispersion-corrected functionals have been applied to the water-ceria (111) interaction[72] and this increases binding energies by 0.18 eV, so a correction of a similar magnitude could be expected for methanol.

We have examined the interaction of methanol in three configurations at the Ti_2O_4 nanocluster (adsorption at the surface sites is always less favourable) which are molecular, dissociative with the O–H bond broken, and dissociative with the methyl C–H bond broken. The final relaxed adsorption structures are shown in Figure 5. Examining these structures, we see that molecular adsorption is never stable – methanol always dissociates spontaneously into a methoxy fragment that binds with Ti from the cluster and hydrogen that binds to oxygen from the cluster. This adsorption structure has an energy gain of 1.62 eV relative to free methanol and the bare Ti_2O_4–CeO_2 structure, which is significantly larger than at the bare surface. With such a large adsorption energies for methanol at Ti_2O_4–CeO_2 compared to adsorption at the bare ceria (111) surface, a correction for dispersion would not change our overall findings regarding methanol adsorption. When dissociated methanol, with a broken O–H bond, is adsorbed as methoxy and H, we consider two configurations: the methoxy and –OH interact with different Ti atoms and methoxy and –OH interact with the same Ti atom. The former relaxes to the structure shown in Figure 5(a) and the latter adsorption structure relaxes to the structure shown in Figure 5(b) and shows a smaller energy gain of −0.86 eV. Thus, the more stable dissociated adsorption mode shows a preference for the methoxy and H fragments to be separated.

The final dissociatively adsorbed methanol configuration, in which the methyl C–H bond is broken, relaxes to the structure in Figure 5(c), which has an energy gain of −0.99 eV relative to free methanol and the oxide. However, this structure spontaneously relaxed to a free formaldehyde molecule and two OH groups on the nanocluster.

If we start from the structure in Figure 5(a) and move a hydrogen from the methyl group to the neighbouring oxygen on the Ti_2O_4 nanocluster, this structure relaxed to formaldehyde and two OH groups with the same structure that results from breaking the methyl C–H bond. We estimate the barrier for this H migration by displacing the H atom along a line from its starting position in the adsorbed methoxy group to oxygen in Ti_2O_4 and perform a series of constrained optimisations in which the migrating H atom is fixed. Although this does not identify a transition state for the migration of hydrogen, it is nonetheless acceptable for the purposes of this work. The estimated barrier for this process is ∼0.3 eV. Thus, these results show that the modification of ceria (111) surface with a Ti_2O_4 nanocluster can have a significant promoting effect in the ODH of methanol to formaldehyde.

IV. CONCLUSIONS

Surface modified ceria catalysts are of great interest for oxidation reactions such as oxidative dehydrogenation of methanol and CO oxidation. Improving the reactivity of ceria based catalysts for these reactions means that they can be run at lower temperatures and DFT simulations of new structures and compositions are proving valuable in the development of these catalysts.

In this paper, we have examined the reactivity of a novel modified ceria material, namely, a Ti_2O_4 species adsorbed on the ceria (111) and (110) surfaces. Taking the oxygen vacancy formation energy and the energy of hydrogenation as descriptors for the reactivity in oxidation reactions, we find that the oxygen vacancy formation energy in the Ti_2O_4–CeO_2 system is significantly reduced compared with the bare ceria surfaces. Comparison with the literature indicates that the presence of ceria-titania interfaces is of benefit in forming oxygen vacancies and reduced metal centres. Adsorption of H at the Ti_2O_4 moiety is more favourable than at the ceria (111) surface. These results hint at improved activity for CO oxidation and the ODH of methanol to formaldehyde, where the oxygen vacancy formation and C–H bond breaking are key steps.

ACKNOWLEDGMENTS

We acknowledge support from Science Foundation Ireland through the Starting Investigator Research Grant Program, project "EMOIN" Grant No. SFI 09/SIRG/I1620. We also acknowledge computing resources provided by SFI to the Tyndall National Institute and by the SFI and Higher Education Authority Funded Irish Centre for High End Computing. Support from the European Commission for access to the JUROPA computer at FZ-Juelich through the FP7 Research Infrastructures Project PRACE-RI (Contract Nos. RI-261557, RI-283493, and RI-312763) is gratefully acknowledged. We acknowledge support from the European Union (EU) through the COST Action CM1104 "Reducible Oxide Chemistry, Structure and Functions."

[1] A. Trovarelli, *Catalysis by Ceria and Related Materials* (Imperial College, UK, 2002).
[2] A. Trovarelli, Catal. Rev. - Sci. Eng. **38**, 439 (1996).
[3] R. J. Gorte, AIChE J. **56**, 1126 (2010).
[4] L. Vivier and D. Duprez, ChemSusChem **3**, 654 (2010).
[5] M. A. Henderson, C. L. Perkins, M. H. Engelhard, S. Thevuthasan, and C. H. F. Penden, Surf. Sci. **526**, 1 (2003).
[6] L. Chen, P. Fleming, V. Morris, J. D. Holmes, and M. A. Morris, J. Phys. Chem. C **114**, 12909 (2010).
[7] S. Bedrane, C. Descorme, and D. Duprez, Catal. Today **75**, 401 (2002).
[8] W. Li, F. J. Garcia, and E. E. Wolf, Catal. Today **81**, 437 (2003).
[9] M. Nolan and G. W. Watson, J. Phys. Chem. B **110**, 16600 (2006).
[10] M. Huang and S. Fabris, J. Phys. Chem. C **112**, 8643 (2008).
[11] E. Aneggi, J. Llorca, M. Boaro, and A. Trovarelli, J. Catal. **234**, 88 (2005).
[12] K. B. Zhou, X. Wang, X. M. Sun, Q. Peng, and Y. D. Li, J. Catal. **229**, 206 (2005).
[13] G. S. Wong, M. R. Concepcion, and J. M. Vohs, J. Phys. Chem. B **106**, 6451 (2002).
[14] I.-C. Marcu, M. N. Urlan, A. Redey, and I. Sandulescu, C. R. Chim. **13**, 365 (2010).
[15] W. Daniell, A. Ponchel, S. Kuba, F. Anderle, T. Weingand, D. H. Gregory, and H. Knözinger, Top. Catal. **20**, 65 (2002).
[16] P. G. Harrison and W. Daniell, Chem. Mater. **13**, 1708 (2001).
[17] Z. Yang, T. K. Woo, and K. Hermansson, J. Chem. Phys. **124**, 224704 (2006).
[18] W. Y. Hernandez, M. A. Centeno, F. Romero-Sarria, and J. A. Odriozola, J. Phys. Chem. C **113**, 5629 (2009).
[19] S. Imamura, T. Higashihara, Y. Saito, H. Aritani, H. Kanai, Y. Matsumura, and N. Tsuda, Catal. Today **50**, 369 (1999).
[20] H. P. Sun, X. P. Pan, G. W. Graham, H.-W. Jen, R. W. McCabe, S. Thevuthasan, and C. H. F. Penden, Appl. Phys. Lett. **87**, 201915 (2005).
[21] B. M. Reddy, P. Bharali, P. Saikia, A. Kahn, S. Loridant, M. Muhler, and W. Gruenert, J. Phys. Chem. C **111**, 1878 (2007).
[22] R. Dziembaj, M. Molenda, L. Chmielarz, M. Drozdek, M. M. Zaitz, B. Dudek, A. Rafalska-Lasocha, and Z. Piwowarska, Catal. Lett. **135**, 68 (2010).
[23] D. R. Ou, T. Mori, F. Ye, T. Kobayashi, J. Zuo, G. Auchterlonie, and J. Drennan, Appl. Phys. Lett. **89**, 171911 (2006).
[24] G. Dutta, U. V. Waghmare, T. Baidya, M. S. Hegde, K. R. Priolkar, and P. R. Sarode, Catal. Lett. **108**, 165 (2006).
[25] G. Dutta, U. V. Waghmare, T. Baidya, M. S. Hegde, K. R. Priolkar, and P. R. Sarode, Chem. Mater. **18**, 3249 (2006).
[26] H. Kadowaki, N. Saito, H. Nishiyama, and Y. Inoue, Chem. Lett. **36**, 440 (2007).
[27] Z.-P. Liu, S. J. Jenkins, and D. A. King, Phys. Rev. Lett. **94**, 196102 (2005).
[28] C. Zhang, A. Michaelides, D. A. King, and S. J. Jenkins, J. Phys. Chem. C **113**, 6411 (2009).
[29] M. Nolan, J. Phys. Chem. C **113**, 2425 (2009).
[30] I. Yeriskin and M. Nolan, J. Phys. Condens. Matter **22**, 135004 (2010).
[31] W. Tang, Z. Hu, M. Wang, G. D. Stucky, H. Metiu, and E. W. McFarland, J. Catal. **273**, 125 (2010).
[32] P. Panagiotopoulou and D. I. Kondarides, Catal. Today **112**, 49 (2006).
[33] M. Flytzani-Stephanopoulos and B. C. Gates, Annu. Rev. Chem. Biomol. Eng. **3**, 545 (2012).
[34] Z. Yang, Q. Wang, and S. Wei, Phys. Chem. Chem. Phys. **13**, 9363 (2011).
[35] G. N. Vayssilov, Y. Lykhach, A. Migani, T. Staudt, G. P. Petrova, N. Tsud, T. Skala, A. Bruix, F. Illas, K. C. Prince, V. Matolin, K. M. Neyman, and J. Libuda, Nature Mater. **10**, 310 (2011).
[36] A. Khodakov, B. Olthof, A. T. Bell, and E. Iglesia, J. Catal. **181**, 205 (1999).
[37] H. L. Abbott, A. Uhl, M. Baron, Y. Lei, R. J. Meyer, D. Stacchiola, O. Bondarchuk, S. Shaikhutdinov, and H. J. Freund, J. Catal. **272**, 82 (2010).
[38] S. Agnoli, M. Sambi, G. Granozzi, C. Castellarin-Cudioa, S. Surnev, M. G. Ramsey, and F. P. Netzer, Surf. Sci. **562**, 150 (2004).
[39] M. Della Negra, M. Sambi, and G. Granozzi, Surf. Sci. **494**, 213 (2001).
[40] M. Baron, H. L. Abbott, O. Bondarchuk, D. Stacchiola, A. Uhl, S. Shaikhutdinov, H.-J. Freund, C. Popa, M. V. Ganduglia-Pirovano, and J. Sauer, Angew. Chem., Int. Ed. **48**, 8006 (2009).
[41] C. Popa, M. V. Ganduglia-Pirovano, and J. Sauer, J. Phys. Chem. C **115**, 7399 (2011).
[42] M. V. Ganduglia-Pirovano, C. Popa, J. Sauer, H. Abbott, A. Uhl, M. Baron, D. Stacchiola, O. Bondarchuk, S. Shaikhutdinov, and H.-J. Freund, J. Am. Chem. Soc. **132**, 2345 (2010).
[43] M. D. Argyle, K. Chen, A. T. Bell, and E. Iglesia, J. Phys. Chem. B **106**, 5421 (2002).
[44] B. Kilos, A. T. Bell, and I. Iglesia, J. Phys. Chem. C **113**, 2830 (2009).
[45] J. N. Brønsted, Chem. Rev. **5**, 231 (1928).
[46] M. G. Evans and M. Polanyi, Trans. Faraday Soc. **34**, 11 (1938).
[47] H. Y. Kim, H. M. Lee, R. G. S. Pala, V. Shapovalov, and H. Metiu, J. Phys. Chem. C **112**, 12398 (2008).
[48] J. Sauer and J. Doebler, Dalton Trans. **2004**, 3116.
[49] J. A. Rodriguez, J. Evans, J. Graciani, J. B. Park, P. Liu, J. Hrbek, and J. Fdez. Sanz, J. Phys. Chem. C **113**, 7364 (2009).
[50] J. B. Park, J. Graciani, J. Evans, D. Stacchiola, S. Ma, P. Liu, A. Nambu, J. F. Sanz, J. Hrbek, and J. A. Rodriguez, Proc. Natl. Acad. Sci. U.S.A. **106**, 4975 (2009).
[51] J. Graciani, J. J. Plata, J. F. Sanz, P. Liu, and J. A. Rodriguez, J. Chem. Phys. **132**, 104703 (2010).
[52] J. B. Park, J. Graciani, J. Evans, D. Stacchiola, S. D. Senanayake, L. Barrio, P. Liu, J. F. Sanz, J. Hrbek, and J. A. Rodriguez, J. Am. Chem. Soc. **132**, 356 (2010).
[53] Y. Fan, Y. M. Choi, S. Agnoli, P. Liu, D. Stacchiola, J. Hrbek, and J. A. Rodriguez, J. Phys. Chem. C **115**, 23062 (2011).
[54] J. A. Rodriguez and D. Stacchiola, Phys. Chem. Chem. Phys. **12**, 9557 (2010).
[55] A. C. Johnston-Peck, S. D. Senanayake, J. J. Plata, S. Kundu, W. Xu, L. Barrio, J. Graciani, J. F. Sanz, R. M. Navarro, J. L. G. Fierro, E. A. Stach, and J. A. Rodriguez, J. Phys. Chem. C **117**, 14463 (2013).
[56] G. Kresse and J. Hafner, Phys. Rev. B **49**, 14251 (1994); G. Kresse and J. Furthmüller, Comput. Mater. Sci. **6**, 15 (1996).
[57] P. E. Blöchl, Phys. Rev. B **50**, 17953 (1994); D. Joubert and G. Kresse, *ibid.* **59**, 1758 (1999).
[58] J. P. Perdew, K. Burke, and M. Ernzerhof, Phys. Rev. Lett. **77**, 3865 (1996).
[59] V. I. Anisimov, J. Zaanen, and O. K. Andersen, Phys. Rev. B **44**, 943 (1991).
[60] S. L. Dudarev, G. A. Botton, S. Y. Savrasov, C. J. Humphreys, and A. P. Sutton, Phys. Rev. B **57**, 1505 (1998).
[61] B. J. Morgan and G. W. Watson, Surf. Sci. **601**, 5034 (2007).
[62] P. A. Mulheran, M. Nolan, C. S. Browne, M. Basham, E. Sanville, and R. A. Bennett, Phys. Chem. Chem. Phys. **12**, 9763 (2010).
[63] M. Nolan, S. C. Parker, and G. W. Watson, Surf. Sci. **595**, 223 (2005).
[64] P. R. L. Keating, D. O. Scanlon, B. J. Morgan, N. M. Galea, and G. W. Watson, J. Phys. Chem. C **116**, 2443 (2012).
[65] J. J. Plata, A. M. Márquez, and J. F. Sanz, J. Chem. Phys. **136**, 041101 (2012).
[66] P. W. Tasker, J. Phys. C **12**, 4977 (1979).
[67] A. Iwaszuk and M. Nolan, Phys. Chem. Chem. Phys. **13**, 4963 (2011).
[68] G. Henkelman, A. Arnaldsson, and H. Jónsson, Comput. Mater. Sci. **36**, 354 (2006).
[69] D. Knapp and T. Ziegler, J. Phys. Chem. C **112**, 17311 (2008).
[70] A. Beste, D. R. Mullins, S. H. Overbury, and R. J. Harrison, Surf. Sci. **602**, 162 (2008).
[71] D. Mei, N. A. Deskins, M. Dupuis, and Q. Ge, J. Phys. Chem. C **112**, 4257 (2008).
[72] D. Fernández-Torre, K. Kośmider, J. Carrasco, M. V. Ganduglia-Pirovano, and R. Pérez, J. Phys. Chem. C **116**, 13584 (2012).